

Synthesis and Characterization of Alumina-Zirconia Powders Obtained by Sol-Gel Method: Effect of Solvent and Water Addition Rate

Julio Del Angel^{1*}, Alberto F. Aguilera¹, Ignacio R. Galindo¹, Merced Martínez², Tomas Viveros³

¹Department of Chemical Engineering, University of Guanajuato, Guanajuato, Mexico; ²Department of Chemistry, University of Guanajuato, Guanajuato, Mexico; ³Department of Chemical Engineering, Metropolitan Autonomous University, Mexico City, Mexico.

Email: *jasoto@ugto.mx, alaguile@ugto.mx

Received June 19th, 2012; revised July 20th, 2012; accepted August 17th, 2012

ABSTRACT

The influence of solvent and the rate of addition of water on the characteristics of alumina-zirconia powders obtained by sol-gel method were investigated. The Al₂O₃-ZrO₂ powders (1:1 molar ratio) were prepared using aluminum tri-sec-butoxide and zirconium n-propoxide as precursors. Ethanol (EtOH), isopropanol (iPrOH) and isobutanol (iBuOH) were used as solvents. The Al₂O₃-ZrO₂ powders were characterized by nitrogen physisorption (S_{BET}), Fourier transformed infrared spectroscopy (FT-IR), thermogravimetric analysis (TGA), differential thermal analysis (DTA), X-ray diffraction (XRD) and scanning electron microscopy (SEM). Prepared oxides calcined at 700°C showed high specific surface area (200 - 240 m²/g). Obtained results suggest that the homogeneity of the mixed oxides is favored by using a water addition rate of 0.06 and 0.10 mL/min with ethanol as solvent.

Keywords: Alumina-Zirconia; Mixed Oxides; Sol Gel Method; Effect of Solvent; Water Addition Rate

1. Introduction

The application of Al₂O₃-ZrO₂ mixed oxides on CH₄ steam reforming reactions has been investigated in recent years [1-3]. Alumina is the most widely known catalyst support for naphtha reforming reactions in the industry; however, catalysts supported on alumina tend to deactivate rapidly by coke formation, which in turn yields less active sites on the surface of the catalyst, consequently decreasing its lifespan [4]. Zirconium oxide is thermally and chemically more stable than aluminum oxide. It is a unique oxide because it possesses acid-base properties [5]. Furthermore, by mixing it with other oxides (Cerium oxide, Lanthanum Oxide, etc.), it presents reducing and oxidizing capabilities [6].

The metal used in the active phase of the catalyst may take different reaction routes when present on other oxides as support, therefore offering the possibility of reducing the undesirable sub-product formation such as coke or acetaldehyde. Furthermore, the complete conversion of hydrocarbons is essential for the reforming process to be cost effective. The catalyst has an important role in attaining such status. Once the rate of the reaction is confirmed by working more efficiently, the system yields more

desired products. Thus, the selection and composition of the catalytic support have a vital consideration in the hydrocarbons' steam reforming reactions [7,8].

The properties of mixed oxides depend on several synthesis parameters: The type of precursor, solvent, water content, pH, precursor concentration, calcination temperature, mechanical or magnetic agitation, speed of agitation, preparation method and type of catalyst [9-12]. Several methods for the synthesis of oxides are reported in the literature. Some of them are: Co-precipitation, sol-gel and calcination [13,14]. The reported advantages in using the sol-gel method are: 1) Large specific surface area; 2) Uniform pore size distribution; 3) Superior homogeneity and purity; 4) High degree of thermal and chemical stability for the supported metals; 5) Better mechanical resistance and 6) Better microstructural control for metallic cluster-formation [15,16].

Several researchers have used the sol-gel method to synthesize Al₂O₃-ZrO₂ powders [17-21]. Chen *et al.* [17,18] have prepared Al₂O₃-ZrO₂ powders with various ZrO₂ contents using the sol-gel route and the co-precipitation method as well. They reported that the powders obtained by the sol-gel route yielded larger surface areas, diameters and smaller pore-sizes than the powders obtained by the co-precipitation method. The surface area of the powders

*Corresponding author.

obtained by the sol-gel route was about twice as large as the powders made by the co-precipitation method, observing that the catalyst effect decreases by increasing the calcination temperatures. The $\text{Al}_2\text{O}_3\text{-ZrO}_2$ mixed oxides with a zirconia content of about 10 wt%, obtained by the sol-gel technique calcined at 700°C has a specific surface area of $290\text{ m}^2/\text{g}$. The specific surface area decreased by increasing the zirconia content. Moreover, the average pore size for the alumina-zirconia powders is affected positively by the relative amount of zirconia incorporated into the mixed oxides synthesis.

Moran-Pineda *et al.* [19] have reported the synthesis and characterization of $\text{Al}_2\text{O}_3\text{-ZrO}_2$ mixed oxides with 5, 10, and 20 wt% of zirconia by the sol-gel method. Their experimental results showed that the oxides, 299, 283 and $354\text{ m}^2/\text{g}$ had relative specific surface areas of 5, 10 and 20 wt% respectively at 500°C . According to their study, the specific surface area increased from 283 to $354\text{ m}^2/\text{g}$ for the mixed oxides at 10 - 20 wt% of zirconia, opposite from the results obtained by Chen *et al.*, who reported that when zirconia goes from 10% to 20%, the surface area decreased from 330 to $290\text{ m}^2/\text{g}$ at 500°C .

Klimova *et al.* [20] investigated a series of $\text{Al}_2\text{O}_3\text{-ZrO}_2$ mixed oxides with variable amounts of ZrO_2 calcined at 300°C , 400°C , 600°C and 800°C . They observed that the specific surface area of mixed oxides at 600°C , with a molar ratio $X = 0.2 (\text{ZrO}_2 / (\text{ZrO}_2 + \text{Al}_2\text{O}_3))$ was about $389\text{ m}^2/\text{g}$, whereas the pure alumina sample yielded a surface area of $349\text{ m}^2/\text{g}$, which suggested that the incorporation of small amounts of zirconia into alumina presumably would increase the specific surface area, but the area actually decreased when more zirconium was added to the alumina. Likewise, smaller average diameter pores in the mixed oxides were obtained when the molar relation increased in comparison with the pure alumina oxide.

Dominguez *et al.* [21] prepared a series of $\text{Al}_2\text{O}_3\text{-ZrO}_2$ solid solutions at different molar ratios. The results obtained by these authors showed that when calcined at 550°C , the mixed oxides had a specific surface area of between 200 and $250\text{ m}^2/\text{g}$. A maximum specific surface area was obtained with a molar ratio $X = 0.2$. Their results agreed with those obtained by Klimova *et al.* [20].

In the synthesis and characterization of $\text{Al}_2\text{O}_3\text{-ZrO}_2$ mixed oxides obtained by the sol-gel method, the supports were prepared using several solvents and different chemical precursors by modifying the process reported by Yoldas [22] for the synthesis of alumina by the sol-gel route.

In the present research, the objective is to investigate the effect of three different solvents on the textural and chemical properties of $\text{Al}_2\text{O}_3\text{-ZrO}_2$, synthesized by the sol-gel method. The effect of four different water-addition rates was also investigated. The lowest value of the water-addition rates resulted in a homogeneous pore-size distribution. The research will allow the development of tai-

lor-made supports to be used in particular hydrocarbon reactions.

2. Experimental

2.1. Procedure

In the present study, $\text{Al}_2\text{O}_3\text{-ZrO}_2$ supports (1:1 molar ratio) were obtained by the sol-gel method, using a molar ratio of 80/30/0.3/1 (alcohol/water/acid/alkoxide). Aluminum tri-sec-butoxide (ATB, 97%, Aldrich) and anhydrous ethanol (94.2% J. T. Baker) were mixed in a reactor vessel with continuous stirring for 20 minutes under an inert atmosphere of nitrogen. In another reactor vessel zirconium (IV) propoxide (ZrP, 70 wt%, Aldrich) and the appropriate amount of ethanol were mixed under an inert atmosphere of nitrogen and then finally stirred for 20 minutes. Afterwards, both solutions were blended, by stirring the mixture vigorously for two hours until a clear solution at room temperature was obtained. An aqueous solution of HNO_3 (65%, J. T. Baker) was added at four addition rates (0.06, 0.1, 0.15 and 0.26 mL/min) to the reactor vessel containing the solution of ethanol and alkoxides under continuous stirring. The gel was aged for 24 hours and dried in a vacuum oven. The starting heat treatment step consisted in drying the powder to 120°C for 1 hour at a heating rate of $1^\circ\text{C}/\text{min}$ starting from room temperature. The resulting powder was finally calcined up to 700°C for 2 hours at a heating rate of $0.5^\circ\text{C}/\text{min}$. **Figure 1** shows the schematic diagram for the experimental set-up for the preparation of $\text{Al}_2\text{O}_3\text{-ZrO}_2$ supports by the sol-gel method. The same procedure was used for the mixed oxides obtained with isopropanol and isobutanol.

2.2. Characterization

The mixed-oxide supports were characterized using a variety of techniques, which are mentioned below.

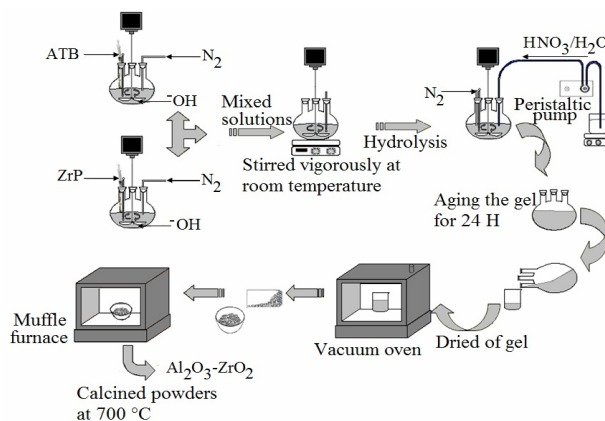


Figure 1. Schematic diagram of experimental set-up for the preparation of $\text{Al}_2\text{O}_3\text{-ZrO}_2$ supports by the sol-gel method.

2.2.1. N₂ Adsorption-Desorption

The specific surface areas of the calcined samples were calculated from N₂ adsorption-desorption acquired data at liquid N₂ temperature on a Micromeritics ASAP 2010 instrument, and the pore size distributions were determined by the Barrett-Joyner-Halenda (B-J-H) method applied to the desorption profile-branch of the nitrogen isotherm.

2.2.2. Infrared Spectroscopy

FT-IR spectroscopy was performed with Perkin Elmer Spectrum 100 equipment on pellets of the mixed oxides at the 400 - 4000 cm⁻¹ wave number range. For this analysis the pellets were elaborated by the application of mechanical pressure on the powdered material formed by adding KBr to the samples to be analyzed.

2.2.3. X-Ray Diffraction

The crystalline degree of the materials was determined by a Kristalloflex Siemens D5000 instrument using monochromatic Cu-K α radiation, scanning 2 θ from 10° to 90°, using standard procedure.

2.2.4. Thermogravimetric Analysis

The thermogravimetric (TGA) and differential thermal (DTA) analyses of Al₂O₃-ZrO₂ mixed oxides were carried out with a heating rate of 10°C/min up to 1000°C in air at 100 mL/min, using a SDT Q600 simultaneous TGA-DSC instrument.

2.2.5. Scanning Electron Microscopy

In this case, the microstructure of the Al₂O₃-ZrO₂ mixed oxides was observed in a Leica S-420 σ scanning electron microscope (SEM) with an acceleration voltage of 20 KeV. The samples were first covered with Au-Pd in a diode sputtering coater

3. Results and Discussions

3.1. Results

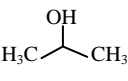
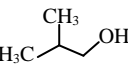
3.1.1. Textural Properties of Supports

Table 1 gives the textural measured properties of the Al₂O₃-ZrO₂ supports (1:1 molar relation) calcined at 700°C. The BET surface areas of 240, 233 and 201 m²/g for ethanol, isopropanol and isobutanol, respectively, were obtained at a water addition rate of 0.06 mL/min. In **Table 1**, it is possible to observe that the surface area decreased with the increase of the water addition rate.

Figure 2 shows the pore size distribution of Al₂O₃-ZrO₂ supports prepared with ethanol, isopropanol and isobutanol. The mean pore size distribution observed at the inset plot of **Figure 2** corresponds to that of a mesoporous material.

The average pore diameter was observed to decrease

Table 1. Textural measured properties of Al₂O₃-ZrO₂ calcined at 700°C.

Solvent	Water addition rate mL/min	S _{BET} (m ² /g)	D _p (Å)	V _p (cm ³ /g)
CH ₃ CH ₂ OH	0.06	240	69	0.47
	0.1	230	60	0.45
	0.15	205	53	0.43
	0.26	165	48	0.41
	0.06	233	88	0.54
	0.10	221	76	0.52
	0.15	200	54	0.48
	0.26	152	73	0.42
	0.06	201	88	0.45
	0.1	198	81	0.40
	0.15	185	80	0.35
	0.26	164	77	0.32

from 69 Å to 48 Å using ethanol as solvent. In the case of the isopropanol used as solvent, the average pore diameter decreased from 88 Å to 54 Å. This effect is observed when isobutanol is used as solvent as well.

The pore size distribution of the mixed oxides observed in **Figure 2(c)** shows a bimodal size distribution, with the first maxima around 27 Å to 35 Å, but when isobutanol alcohol is used as solvent, a second maxima is observed around 60 Å to 100 Å for all water addition rates. The pore size distribution analysis of **Figures 2(a)** and **(b)** suggests that for a water addition rate of 0.06 mL/min a bimodal pore size distribution is obtained when the mixed oxides are prepared using ethanol and isopropanol as solvents. The remaining water-addition rates for the latter solvents present only a monomodal pore size distribution.

The nitrogen adsorption-desorption isotherms of Al₂O₃-ZrO₂ supports were prepared with ethanol, isopropanol and isobutanol, which are shown in **Figure 3**.

The supports show E-type hysteresis loops, which are interpreted as type IV isotherms, indicating the probable existence of tubular pores with narrow openings or tubular pores with irregular narrow openings, otherwise known as ink-well type pores.

3.1.2. FT-IR Analysis

Figure 4 shows spectra obtained by means of FT-IR analyses of Al₂O₃-ZrO₂ supports calcined at 700°C prepared with ethanol as solvent at two water-addition rates. Similar results were obtained using isopropyl and isobutyl alcohols as solvents.

The FT-IR spectra in the 4000 - 2900 cm⁻¹ region show a broad band for the two water addition rates, a characteristic assigned to the presence of structural OH⁻ groups. One band is observed at 3442 cm⁻¹ for the water-addition rate of 0.06 mL/min is shown in **Figure 4(a)**, while the other band appears at 3447 cm⁻¹ for the water-addition

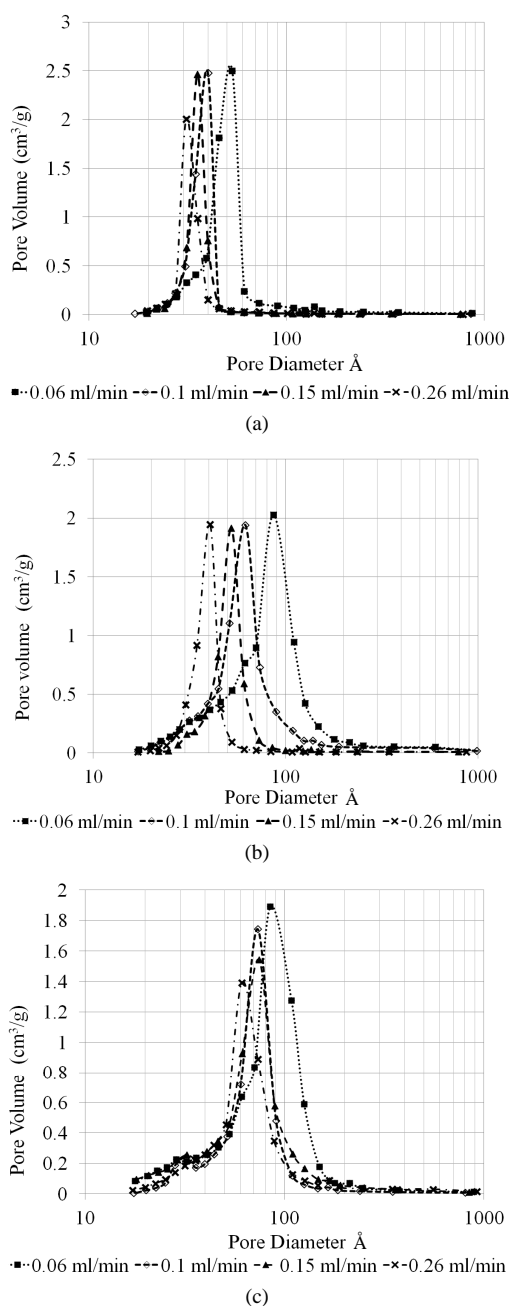


Figure 2. Pore size distribution of $\text{Al}_2\text{O}_3\text{-ZrO}_2$ supports prepared with (a) Ethanol; (b) Isopropanol; and (c) Isobutanol, obtained using different water addition rates.

rate of 0.26 mL/min is shown in **Figure 4(b)**. A small extra band is observed at 2900 cm^{-1} for the water-addition rate of 0.26 mL/min, which is assigned to C-H vibration due to an incomplete polymerization, whereas this band is not observed at the lower water-addition rate [19,23]. The band associated with the stretching vibrations for the Zr-O-Al bond appears at 2374 cm^{-1} at the water addition rate of 0.26 mL/min. The band decrease in the $\text{Al}_2\text{O}_3\text{-ZrO}_2$ mixed oxides obtained

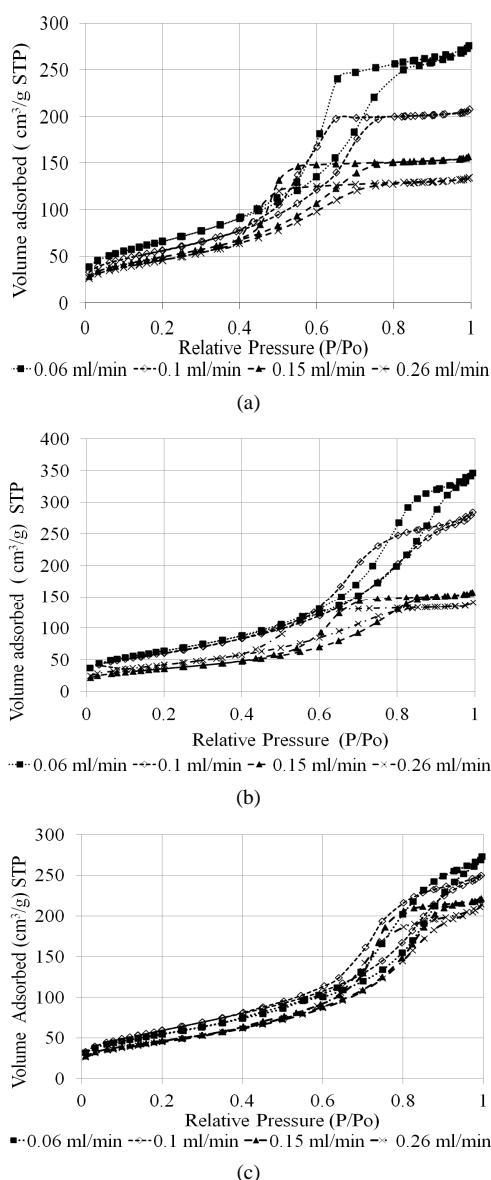


Figure 3. Adsorption-desorption isotherms of the $\text{Al}_2\text{O}_3\text{-ZrO}_2$ supports prepared with (a) Ethanol; (b) Isopropanol; and (c) Isobutanol, obtained from different water addition rates.

from a low water-addition rate is due to lattice structural rearrangement. The bending vibrations of Zr-OH bonds appear at $1630 - 1631\text{ cm}^{-1}$ for both hydrolysis rates [24]. The bands appearing at 1395 and 1407 cm^{-1} are typical for the γ -alumina support. The Al-O vibration is observed at 1371 and 1363 cm^{-1} for a water-addition rate of 0.06 and 0.26 mL/min respectively. Another important adsorption band can be observed at 523 cm^{-1} , which corresponds to the vibration of the Zr-O-Al bond in the alumina-zirconia powders [25].

3.1.3. X-Ray Diffraction

The XRD spectra of the $\text{Al}_2\text{O}_3\text{-ZrO}_2$ supports at different

water-addition rates are presented in **Figure 5**. The spectra of the Al_2O_3 , **Figure 5(a)** support showed typical diffraction peaks of γ -Alumina. This fact indicates that the synthesized alumina is apparently amorphous. Two small lumps are observed at $2\theta - 46^\circ$ and $2\theta - 66^\circ$ that can also be related to an incipient ordered structure.

The peak corresponding to the ZrO_2 phase in supports

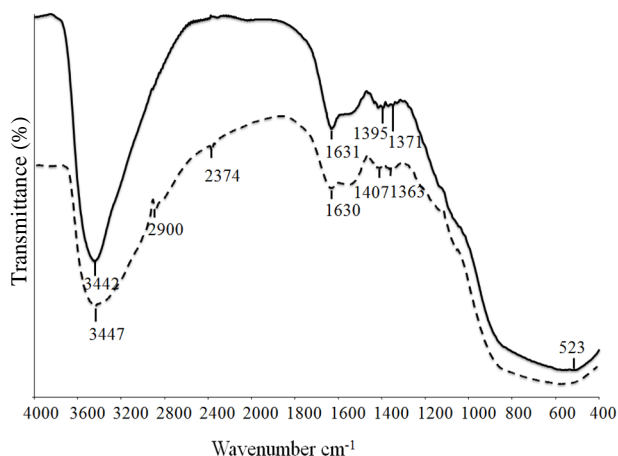


Figure 4. FT-IR spectra of the $\text{Al}_2\text{O}_3\text{-ZrO}_2$ supports prepared with ethanol, which were calcined at 700°C for (a) 0.06 ml/min (—) and (b) 0.26 ml/min water addition rates (- -).

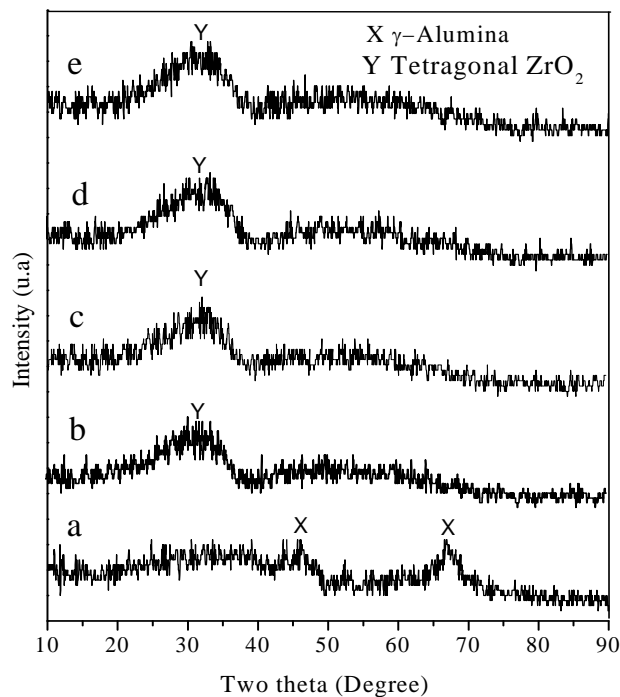


Figure 5. XRD spectra of $\text{Al}_2\text{O}_3\text{-ZrO}_2$ supports at different water addition rates (a) Al_2O_3 ; (b) $\text{Al}_2\text{O}_3\text{-ZrO}_2$ 0.06 ml/min ; (c) $\text{Al}_2\text{O}_3\text{-ZrO}_2$ 0.1 ml/min ; (d) $\text{Al}_2\text{O}_3\text{-ZrO}_2$ 0.15 ml/min ; (e) $\text{Al}_2\text{O}_3\text{-ZrO}_2$ 0.26 ml/min , using ethanol as solvent, calcined at 700°C .

spectra for $\text{Al}_2\text{O}_3\text{-ZrO}_2$ is not detectable; however a moderate plateau of tetragonal ZrO_2 is shown at $2\theta - 30^\circ$, indicating the presence of an incipient crystalline structure in the synthesized mixed oxides [26,27]. This incipient crystalline structure is responsible for the low level definition of the bands at 523 cm^{-1} and 525 cm^{-1} in the FT-IR studies [27].

3.1.4. Thermogravimetric Analysis

The TGA-DTA curves of the fresh $\text{Al}_2\text{O}_3\text{-ZrO}_2$ mixed oxides are shown in **Figure 6** using ethanol as solvent. For a water-addition rate of 0.06 ml/min , **Figure 6(a)**: One zone of the DTA curve in the temperature range $21^\circ\text{C} - 180^\circ\text{C}$ corresponds to an endothermic change leading to dehydration of $\text{Al}_2\text{O}_3\text{-ZrO}_2$ powders. Likewise, the zone in the temperature range $180^\circ\text{C} - 250^\circ\text{C}$ is exothermic and can be attributed to the incipient combustion of organic groups. In the third decomposition zone which is exothermic, in the temperature range $250^\circ\text{C} - 291^\circ\text{C}$, corresponds to the elimination of chemically bonded water [19,20,27]. The fourth decomposition zone in the temperature range $291^\circ\text{C} - 374^\circ\text{C}$ corresponds to the total combus-

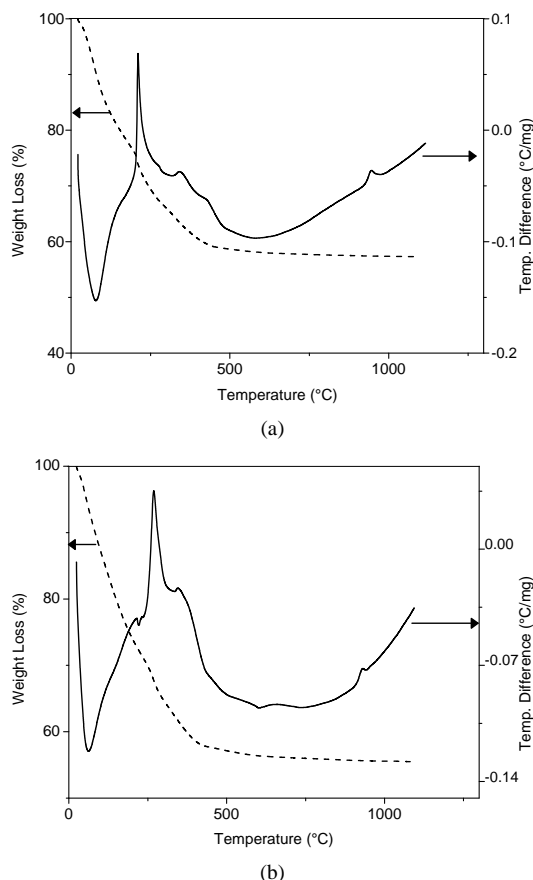


Figure 6. TGA-DTA thermograms of $\text{Al}_2\text{O}_3\text{-ZrO}_2$ supports for the water-addition rates of: (a) 0.06 ml/min ; (b) 0.26 ml/min , using ethanol as solvent. TGA (- -), DTA (—).

tion of organic compounds. The exothermic small peak in the temperature range 374°C - 481°C is observed in the DTA curve. This signal is associated with the tetragonal phase ZrO₂. A zone in the temperature range 481°C - 637°C corresponds to an endothermic change due to the conversion of dehydroxylated boehmite to γ -Al₂O₃ [28]. Finally, in the temperature range 850°C - 1091°C there is an exothermic change, which is caused by the transformation of the ZrO₂ tetragonal phase to a monoclinic phase.

For the water addition rate of 0.26 mL/min, **Figure 6(b)**: A first zone of the DTA curve in the temperature range 21°C - 109°C is due to the evaporation of adsorbed water from the Al₂O₃-ZrO₂ powders. A second zone in the temperature range 109°C - 234°C is exothermic and can be attributed to a total dehydration of mixed oxides and to the incipient combustion of the organic groups. In the third decomposition zone which is exothermic, in the temperature range 234°C - 304°C, the peak corresponds to the elimination of chemically bonded water. The fourth decomposition zone in the temperature range 304°C - 451°C corresponds to the total combustion of organic compounds [19,26,27]. A fifth zone in the temperature range 451°C - 678°C is associated to an endothermic change due to the conversion of dehydroxylated boehmite to γ -Al₂O₃ [24]. Finally, in the temperature range 850°C - 1091°C, there is an exothermic change, which is caused by the transformation of the tetragonal into the monoclinic zirconia phase.

3.1.5. Scanning Electron Microscopy

Figure 7 shows the micrographs obtained from the scanning electron microscopy studies for the Al₂O₃-ZrO₂ powders where an appreciable formation of agglomerates can be seen. The results show that the particle size increased by increasing the water addition rate. The agglomerates are composed of mostly homogeneous-sized particles as can be observed in **Figure 7(a)** for the 0.06 mL/min water-addition rate. On the other hand, **Figure 7(b)**, shows a dispersion of non-spherical particles, where serrated edges are observed for the 0.26 mL/min water-addition rate. The lowest water-addition rate allowed for a higher extent of polymerization due to a longer reaction time which yielded more homogenous-sized particles. At the largest water-addition rate, the polymerization extent was less complete due to both the greater amount of reactant and less reaction time, which yielded particles that were less rounded and had a lesser degree of aggregation.

3.2. Discussions

The main difference observed when using three different solvents was related to the textural properties of the materials. The use of ethanol as solvent achieved a narrow pore-size distribution centered at the lowest pore-diameter

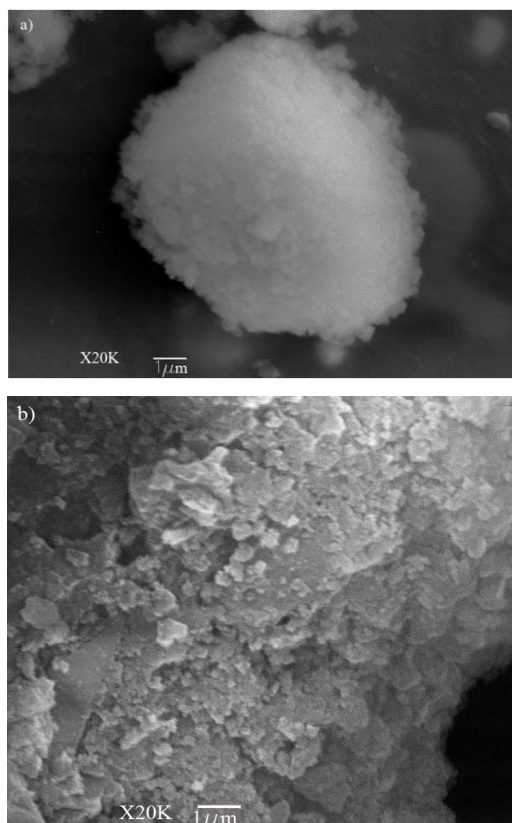


Figure 7. Micrograph by SEM (20,000x magnification) of the Al₂O₃-ZrO₂ support (calcined at 700°C) obtained with ethanol as solvent at a water addition rate of a) 0.06 mL/min; b) 0.26 mL/min.

and with the highest surface area suitable for reactions where small molecules can participate. On the other hand, the use of isobutanol as solvent generated the highest average-pore diameter, yielding consequently the lowest surface area. The FT-IR, TGA-DTA and XRD analyses were obtained for all solvents, and the main features are described only for ethanol in this contribution, since the remaining solvents show equivalent behavior.

As the water-addition rate was increased the BET surface area decreased, this effect is confirmed by SEM micrographs where particle-agglomeration is observed, **Figure 7(b)**. The latter concept is further confirmed by the FT-IR analysis when a water-addition rate of 0.26 mL/min is used, where a less intense peak at 3447 cm⁻¹ associated to surface OH⁻ groups indicates a larger agglomeration degree. The presence of an FT-IR signal at 2900 cm⁻¹ associated to C-H vibrations indicates an incomplete polymerization assumed to be due to a short reaction time. The TGA-DTA analysis shows a larger zone at 300°C - 450°C with respect to the lower water-addition rate in **Figure 6**, which indicates the presence of more chemically-bound hydrocarbons from non-reacted alkoxides, as verified by the FT-IR analysis.

The BET surface area determined at a water-addition rate of 0.06 mL/min is larger when using ethanol as solvent. The micrograph by SEM reveals in this case the formation of uniform-sized particles with facile agglomeration and no appreciable distortions. The agglomeration of small spherical particles generates an E-type hysteresis loop, confirmed by the N₂ adsorption determination. It is proposed that such configuration was achieved by a combination of variables; time is important during particle formation while the textural properties are affected by the solvent. Lower water-addition rates facilitate the growth of completely-polymerized particles. TGA-DTA analysis indicates the formation and particle agglomeration with minor incorporation of non-reacted components, which can be observed by a lesser weight loss in the range 300°C - 450°C than that observed at the larger water-addition rate. The FT-IR signal at 3442 cm⁻¹ associated to OH⁻ groups is more intense. The latter has been ascribed to a larger concentration of OH⁻ groups, tied to a higher degree of polymerization that turns out in a lack of C-H vibrations at 2900 cm⁻¹ as observed in **Figure 4(a)**.

4. Conclusions

According to the results and discussions, the following conclusions are:

- 1) The use of ethanol as solvent produced Al₂O₃-ZrO₂ mixed oxides with higher specific surface internal areas than employing isopropyl or isobutyl alcohols;
- 2) The average pore diameter is largest in this study when isobutyl alcohol is used as solvent for the synthesized Al₂O₃-ZrO₂ supports;
- 3) High pore volumes were favored by using the isopropyl alcohol as solvent to the obtained Al₂O₃-ZrO₂ mixed oxides;
- 4) The water-addition rate of 0.26 mL/min leads to significant structural changes as indicated by the analysis of the FT-IR spectra, which can be attributed to an incomplete polymerization in the synthesis of the supports;
- 5) X-ray diffraction patterns for all samples do not identify well-defined crystalline structures corresponding to ZrO₂ or Al₂O₃. This fact suggests that the samples are mostly amorphous solids;
- 6) For water addition at a rate of 0.10 mL/min the specific surface area of Al₂O₃-ZrO₂ powders is almost equal to that obtained at a water-addition rate of 0.06 mL/min, hence, this rate can be used to prepare catalytic supports.

5. Acknowledgements

Julio Del Angel expresses recognition to the University of Guanajuato for the financial support granted to this project and to CONACYT for the scholarship stipend.

REFERENCES

- [1] J. G. Seo, M. H. Youn and K. M. Cho, "Effect of Al₂O₃-ZrO₂ Xerogel Support on Hydrogen Production by Steam Reforming of LNG over Ni/Al₂O₃-ZrO₂ Catalyst," *Korean Journal of Chemical Engineering*, Vol. 25, No. 1, 2008, pp. 41-45. [doi:10.1007/s11814-008-0007-4](https://doi.org/10.1007/s11814-008-0007-4)
- [2] J. G. Seo, M. H. Youn, K. M. Cho, S. Park and I. K. Song, "Preparation of Ni/Al₂O₃-ZrO₂ Catalysts and Their Application to Hydrogen Production by Steam Reforming of LNG: Effect of ZrO₂ Content Grafted on Al₂O₃," *Catalysis Today*, Vol. 138, No. 3-4, 2008, pp. 130-134. [doi:10.1016/j.cattod.2008.05.006](https://doi.org/10.1016/j.cattod.2008.05.006)
- [3] P. Jasso, M. Torres, F. Tzompanzi and M. Asomoza, "Nanostructured Carbon on Steam Reforming Catalysts," *Journal of New Materials for Electrochemical Systems*, Vol. 11, No. 2, 2008, pp. 95-98.
- [4] Q. Liu, A. Wang, X. Wang, P. Gao, X. Wang and T. Zhang, "Synthesis, Characterization and Catalytic Applications of Mesoporous γ -Alumina from Boehmite Sol," *Microporous and Mesoporous Materials*, Vol. 111, No. 1-3, 2008, pp. 323-333. [doi:10.1016/j.micromeso.2007.08.007](https://doi.org/10.1016/j.micromeso.2007.08.007)
- [5] P. D. L. Mercera, J. G. Van Ommen, E. B. M. Doesburg, A. J. Burggraaf and J. R. H. Ross, "Stabilized Tetragonal Zirconium Oxide as a Support for Catalysts," *Applied Catalysis*, Vol. 78, No. 1, 1991, pp. 79-96. [doi:10.1016/0166-9834\(91\)80090-J](https://doi.org/10.1016/0166-9834(91)80090-J)
- [6] M. G. Cutrufello, I. Ferino, R. Monaci, E. Rombi and V. Solin, "Acid-Base Properties of Zirconium, Cerium and Lanthanum Oxides by Calorimetric and Catalytic Investigation," *Topics in Catalysis*, Vol. 19, No. 3-4, 2002, pp. 225-240. [doi:10.1023/A:1015376409863](https://doi.org/10.1023/A:1015376409863)
- [7] C. Bozo, N. Guilhaume, E. Garbowski and M. Primet, "Combustion of Methane on CeO₂-ZrO₂ Based Catalysts," *Catalysis Today*, Vol. 59, No. 1-2, 2000, pp. 33-45. [doi:10.1016/S0920-5861\(00\)00270-4](https://doi.org/10.1016/S0920-5861(00)00270-4)
- [8] A. Haryanto, S. Fernando, N. Murali and S. Adhikari, "Current Status of Hydrogen Production Techniques by Steam Reforming of Ethanol: A Review," *Energy & Fuels*, Vol. 19, No. 5, 2005, pp. 2098-2106. [doi:10.1021/ef0500538](https://doi.org/10.1021/ef0500538)
- [9] A. Srivastava and M. K. Dongare, "Low-Temperature Preparation of Tetragonal Zirconia," *Materials Letters*, Vol. 5, No. 3, 1987, pp. 111-115. [doi:10.1016/0167-577X\(87\)90086-3](https://doi.org/10.1016/0167-577X(87)90086-3)
- [10] P. D. L. Mercera, J. G. Van Ommen, E. B. M. Doesburg, A. J. Burggraaf and J. R. H. Ross, "Zirconia as a Support for Catalysts: Evolution of the Texture and Structure on Calcination in Air," *Applied Catalysis*, Vol. 57, No. 1, 1990, 127-148. [doi:10.1016/S0166-9834\(00\)80728-9](https://doi.org/10.1016/S0166-9834(00)80728-9)
- [11] W. Zhang and F. P. Glasser, "Condensation and Gelation of Inorganic ZrO₂-Al₂O₃ Sols," *Journal of Materials Science*, Vol. 28, No. 4, 1993, pp. 1129-1135. [doi:10.1007/BF00400902](https://doi.org/10.1007/BF00400902)
- [12] M. L. Rojas Cervantes, R. M. Martin-Aranda, A. J. Lopez-Peinado and J. De D. Lopez-Gonzalez, "ZrO₂ Obtained by the Sol-Gel Method: Influence of Synthesis Pa-

- rameters on Physical and Structural Characteristics,” *Journal of Materials Science*, Vol. 29, No. 14, 1994, pp. 3743-3748. [doi:10.1007/BF00357343](https://doi.org/10.1007/BF00357343)
- [13] Z. Feng, W. S. Postula, A. Akgerman and R. G. Anthony, “Characterization of Zirconia-Based Catalysts Prepared by Precipitation, Calcination, and Modified Sol-Gel Methods,” *Industrial & Engineering Chemistry Research*, Vol. 34, No. 1, 1995, pp. 78-82. [doi:10.1021/ie00040a005](https://doi.org/10.1021/ie00040a005)
- [14] V. Naglieri, L. Joly-Pottuz, J. Chevalier, M. Lombardi and L. Montanaro, “Follow-Up of Zirconia Crystallization on a Surface Modified Alumina Powder,” *Journal of the European Ceramic Society*, Vol. 30, No. 16, 2010, pp. 3377-3387. [doi:10.1016/j.jeurceramsoc.2010.07.029](https://doi.org/10.1016/j.jeurceramsoc.2010.07.029)
- [15] K. Balakrishnan and R. D. Gonzalez, “Preparation of Pt/Alumina Catalysts by the Sol-Gel Method,” *Journal of Catalysis*, Vol. 144, No. 2, 1993, pp. 395-413. [doi:10.1006/jcat.1993.1341](https://doi.org/10.1006/jcat.1993.1341)
- [16] R. Gopalan, C. H. Chang and Y. S. Lin, “Thermal Stability Improvement on Pore and Phase Structure of Sol-Gel Derived Zirconia,” *Journal of Materials Science*, Vol. 30, No. 12, 1995, pp. 3075-3081. [doi:10.1007/BF01209219](https://doi.org/10.1007/BF01209219)
- [17] C. Li, Y.-W. Chen and T.-M. Yen, “The Effects of Preparation Method on the Characteristics of Alumina-Zirconia Powders,” *Journal of Sol-Gel Science and Technology*, Vol. 4, No. 3, 1995, pp. 205-215. [doi:10.1007/BF00488375](https://doi.org/10.1007/BF00488375)
- [18] Y.-W. Chen, T.-M. Yen and C. Li, “Preparation of Alumina-Zirconia Materials by the Sol-Gel Method from Metal Alkoxides,” *Journal of Non-Crystalline Solids*, Vol. 185, No. 1-2, 1995, pp. 49-55. [doi:10.1016/0022-3093\(94\)00680-6](https://doi.org/10.1016/0022-3093(94)00680-6)
- [19] M. Morán-Pineda, S. Castillo, T. López, R. Gómez, Cordero-Borboa and O. Novaro, “Synthesis, Characterization and Catalytic Activity in the Reduction of NO by CO on Alumina-Zirconia Sol-Gel Derived Mixed Oxides,” *Applied Catalysis B: Environmental*, Vol. 21, No. 2, 1999, pp. 79-88. [doi:10.1016/S0926-3373\(99\)00010-7](https://doi.org/10.1016/S0926-3373(99)00010-7)
- [20] T. Klimova, M. L. Rojas, P. Castillo, R. Cuevas and J. Ramirez, “Characterization of Al₂O₃-ZrO₂ Mixed Oxide Catalytic Supports Prepared by the Sol-Gel Method,” *Microporous and Mesoporous Materials*, Vol. 20, No. 4-6, 1998, pp. 293-306. [doi:10.1016/S1387-1811\(97\)00024-3](https://doi.org/10.1016/S1387-1811(97)00024-3)
- [21] J. M. Domínguez, J. L. Hernandez and G. Sandoval, “Surface and Catalytic Properties of Al₂O₃-ZrO₂ Solid Solutions Prepared by Sol-Gel Methods,” *Applied Catalysis A: General*, Vol. 197, No. 1, 2000, pp. 119-130.
- [22] B. E. Yoldas, “Alumina Gels That Form Porous Transparent Al₂O₃,” *Journal of Materials Science*, Vol. 10, No. 11, 1975, pp. 1856-1860. [doi:10.1007/BF00754473](https://doi.org/10.1007/BF00754473)
- [23] S. Therdthianwong, A. Siangchin and A. Therdthianwong, “Improvement of Coke Resistence of Ni/Al₂O₃ Catalyst in CH₄/CO₂ Reforming by ZrO₂ Addition,” *Fuel Processing Technology*, Vol. 89, No. 2, 2008, pp. 160-168. [doi:10.1016/j.fuproc.2007.09.003](https://doi.org/10.1016/j.fuproc.2007.09.003)
- [24] D. Sarkar, D. Mohapatra, S. Ray, S. Bhattacharyya, S. Adak and N. Mitra, “Synthesis and Characterization of Sol-Gel Derived ZrO₂ Doped Al₂O₃ Nanopowder,” *Ceramics International*, Vol. 33, No. 7, 2007, pp. 1275-1282. [doi:10.1016/j.ceramint.2006.05.002](https://doi.org/10.1016/j.ceramint.2006.05.002)
- [25] A. Taavani-Gilan, E. Taheri-Nasaj and H. Akhondi, “The Effect of Zirconia Content on Properties of Al₂O₃-ZrO₂ (Y₂O₃) Composite Nanopowders Synthesized by Aqueous Sol-Gel Method,” *Journal of Non-Crystalline Solids*, Vol. 355, No. 4-5, 2009, pp. 311-316. [doi:10.1016/j.jnoncrysol.2008.11.012](https://doi.org/10.1016/j.jnoncrysol.2008.11.012)
- [26] J. Ortiz-Landeros, M. E. Contreras-García and H. Pfeiffer, “Synthesis of Macroporous Al₂O₃-ZrO₂ Mixed Oxides with Mesoporous Walls, Using Polystyrene Spheres as Template,” *Journal of Porous Materials*, Vol. 16, No. 4, 2009, pp. 473-479. [doi:10.1007/s10934-008-9221-z](https://doi.org/10.1007/s10934-008-9221-z)
- [27] V. Santos, M. Zeni, C. P. Bergmann and J. M. Hohemberger, “Correlation between Thermal Treatment and Tetragonal/Monoclinic Nanostructured Zirconia Powder Obtained by Sol-Gel Process,” *Review on Advanced Materials Science*, Vol. 17, No. 1, 2008, pp. 62-70.